Procedia Manufacturing

Volume 1, 2015, Pages 393–403

43rd Proceedings of the North American Manufacturing Research Institution of SME http://www.sme.org/namrc

In-Situ Metrology System for Laser Powder Bed Fusion Additive Process

William S. Land II[1], Bin Zhang[1], John Ziegert[1], and Angela Davies[1]

[1]*The University of North Carolina at Charlotte, Charlotte, NC, USA*

wland1@uncc.edu, bzhang8@uncc.edu, jziegert@uncc.edu, adavies@uncc.edu

Abstract

Complex metal parts produced by additive manufacturing processes are often very difficult to dimensionally characterize by traditional contact and non-contact metrology systems. The most efficient and effective approach to measuring metal additively produced parts, particularly those produced in a laser powder bed fusion process, is to measure each layer of the part as it is sintered. In this layer-wise measurement approach, what are internal and obscured features in the final part are accessible to measurement while the part build is still in process. This paper describes the development of a metrology system which performs non-contact measurement of a nickel powder laser fusion system. The metrology system discussed herein uses a traditional machine vision linear approximation to measure the planar dimensions of each build layer, and a phase shifting fringe projection system to produce an area height profile of each layer. The independent measurements can be combined to produce a high density 3D point cloud of the final part, including all internal and obscured features. This project is ongoing, and results are incomplete.

Keywords: Additive manufacturing, non-contact metrology, in-situ measurement, laser powder bed fusion, SLM

1 Introduction

Improvements in metal additive manufacturing processes have generated massive opportunity for novel engineering within the design and implementation of precision, high functionality components. Many industries aim to take advantage of the assets metal additive manufacturing offers. To fully realize these potential benefits, further improvements are needed in all aspects of additively produced parts, from their metallurgical properties to their dimensional accuracy and surface finish.

One of the many challenges associated with producing high precision parts additively, in particular understanding and improving their dimensional accuracy, is the relative inability to measure them by conventional means after they have been manufactured. Some of the most powerful advantages of producing parts with an additive process are the ability to include atypical geometries and complex internal structures within a design. Both of these hinder efforts to perform metrology on a completed part with many standard measurement tools. Current technologies produce surface finishes that are often much too rough to perform scans with a traditional touch probe without causing

Peer-review under responsibility of the NAMRI Scientific Committee

doi:10.1016/j.promfg.2015.09.047

damage; key features are often obscured from view and inaccessible; internal structures are nearly impossible to measure with almost any contact or non-contact measurement approach outside of x-ray tomography which is very costly and complicated. Simply put, if a part can be readily measured by common devices, whether contact or non-contact, it is likely readily made with a traditional machine tool, and is therefore likely an inappropriate candidate for additive manufacturing due to the current economic disadvantages of the technology. As such, measurements must be carried out during the manufacturing process, while all features are still accessible to probing, in order to fully characterize a part's geometry.

This paper discusses the development of an in-situ measurement process for use specifically within a laser powder bed fusion chamber. The investigation of this particular additive manufacturing process has been motivated by several federal and industrial sponsors, but is largely supported by the America Makes – National Additive Manufacturing Innovation Institute. As a collaborator, Edison Welding Institute in Columbus, Ohio, has built a working open source fusion chamber for the purpose of sensor integration and testing. The laser powder bed fusion process involves the direction of a focused laser beam via a galvanometer laser scanner over a flat bed of metal powder. As the laser beam is manipulated, the area of powder over which it traverses is fused together, forming a thin layer of solid metal. A new layer of powder is then deposited atop the previous layer, and a new area is then exposed to the laser beam. In this fashion a part can be built up layer wise. As a result of the process, the dimensional characteristics of a part are manifested in the boundary between areas that have been fused into solid metal and areas of unfused powder in each layer. Determining this boundary with high fidelity immediately after the lasing of each layer amounts to measuring a profile of the outer surface of the final part at the layer's respective height within the total build. Therefore, determining the solid-powder boundary for every layer sequentially allows for the boundaries of the entire part to be created by digitally stacking the individual layer boundaries, ending in characterization of all surfaces by profile lines at a resolution of the build layer thickness. In addition to mapping each layer of the part as it is being made, monitoring the area height profile of each layer is expected to provide insight into other quality issues such as splatter of molten material, interstitial void formation due to bubbles, and general information on the surface structure of the powder bed.

The approach to measuring each sintered layer described here involves the combination of a traditional machine vision system and a digital fringe projection system. The fringe projection technique is used to calculate the area height profile of each layer, while a machine vision algorithm provides the proper planar mapping from camera pixels to in-plane object coordinates. A schematic of the measurement system as mounted on the laser fusion chamber is shown below in Figure 1. The process involves the use of one digital single-lens reflex (SLR) camera and a digital light processing (DLP) projector. Three cameras have been integrated into the fusion chamber for the purpose of future advancement of the measurement process. The availability to measure the powder surface from multiple angles will provide means for a more robust measurement as the project progresses.

The primary means of determining the solid-powder boundary within each sintered layer of a build is the measurement of the height profile. The laser powder bed fusion system studied here uses IN625 nickel alloy powder as its printing media. The solidification of this particular powder by sintering causes approximately a 40-50% increase in density. Therefore, the powder regions exposed to the laser during sintering will experience a measureable drop in height as compared to the unaltered regions. By comparing the surface profile of a layer after sintering to a baseline area profile of that same layer prior to laser exposure, it is possible to distinguish solidified area from powder by examining relative height change. As noted, the measurement of lateral and vertical coordinates within the powder bed occur independently of each other, and as such, each requires its own calibration and data processing procedure, as will be discussed below.

2 Principle of Operation

2.1 Planar Coordinate Measurement via Machine Vision

Measuring the planar coordinates of locations within the build area is performed through the processing of a single image of each sintered layer. This measurement relies on the linear mapping of pixel coordinates within each image to an established reference coordinate system within the test chamber. The mapping is created through a calibration procedure, and the calibration's stability, and therefore future measurement accuracy, depends on the spatial relationship between the camera and the build plane remaining constant. As such, rigid fixturing is required to maintain image space orientation throughout the entire build process. The measurement process can be broken down into two basic steps, initial calibration and image mapping.

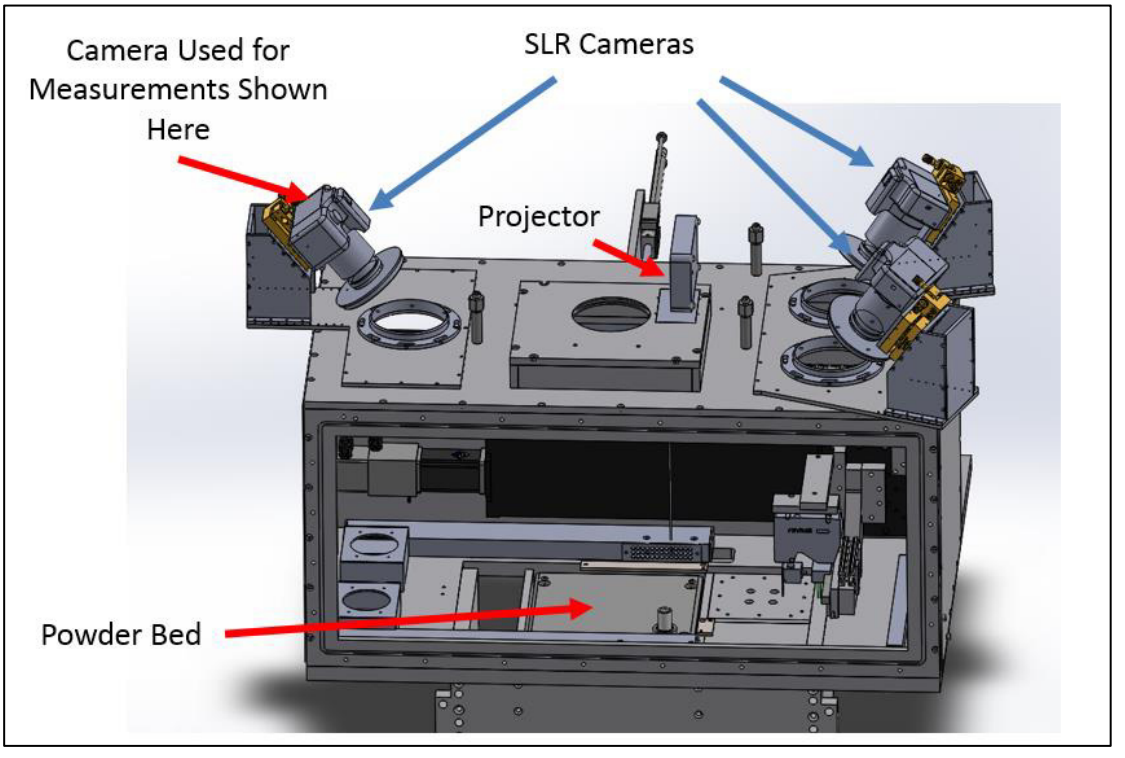

Figure 1: Schematic of measurement systems' integration into the laser powder bed fusion chamber at Edison Welding Institute. The camera used to produce the measurements shown in this paper is that shown on the left of the figure. The remaining two cameras are meant to support future developments in the measurement scheme.

The calibration process requires a grid plate to be used as a reference artifact. The plate contains an 11 x 11 grid of 7.5 mm reamed holes of constant 15 mm 2D pitch, thereby covering an area of 150 x 150 [mm]. The pattern has been measured using a CMM contact probe to establish the hole centers at the upper surface of the plate. This measurement and a measure of its uncertainty is used as the global reference for the creation of both a projective transformation matrix and a linear mapping of orthogonal pixel coordinates to metered space, which collectively define the calibration of the system.

After the CMM measurement of the grid plate, the holes were back filled with a non-expanding epoxy to create a flat upper surface for imaging with high greyscale contrast at the hole edges. To calibrate the measurement system, the grid plate is imaged within the chamber where it fully encompasses the area where powder will be fused. Using linear stages within the chamber, the

reference artifact is positioned so that its upper surface coincides with the focal plane of the laser scanning system, or the "build plane". The image of the grid plate is processed using a contrast thresholding algorithm in order to perform circle fitting to the back filled holes within the plate.

Using the relative center location in pixel coordinates of each hole by means of a least squares circle fit, an inverse projection transformation matrix is calculated using the CMM measured part coordinates of the four corner circles. The projective transformation matrix shown in Eq 1 is the first output of the calibration procedure. It is used to correct perspective warping in the non-orthogonal images taken of the powder bed. The projective transformation $\boldsymbol{T}$ is defined as,

$$\boldsymbol{T} = \begin{bmatrix} a_{11} & a_{12} & a_{13} \\ a_{21} & a_{22} & a_{23} \\ a_{31} & a_{32} & a_{33} \end{bmatrix} \tag{1}$$

such that,

$$[x'\ y'\ w'] = [u\ v\ 1] \cdot \boldsymbol{T} \tag{2}$$

where $[u\ v]$ are coordinates in the original image space, and $[x'/w'\ \ y'/w']$ are coordinates in orthogonal planar object space [Wolberg, 1994]. The transformation matrix calculated from Eq 1 & 2 during the calibration process is saved and used to remove perspective warping in all future images from the system under the assumption that imaging system is geometrically stable. The projection transformation matrix is then applied to the entire calibration image to remove the planar perspective warping. This creates an orthogonal image of the grid plate artifact. An example of a processed and transformed image of a calibration grid is shown below in Figure 2.

After transformation, to create the linear mapping from orthogonal pixel space to metered space, the relative circle centers in the transformed image are compared to their known relative locations as measured by the CMM. The ratio of the two locations gives a map of linear scaling factors in millimeters per pixel at each of the hole locations within the transformed camera image. The mapping is defined as,

$$\boldsymbol{S}_{x,y}(i) = \frac{P_{CMM_{x,y}}(i)}{P_{OrthoImage_{x,y}}(i)}\ [\frac{mm}{pixel}] \tag{3}$$

where applied to future images subsequent to calibration,

$$[x\ y] = \boldsymbol{S} \cdot \left[\frac{x'}{w'}\ \frac{y'}{w'}\right]\ [mm] \tag{4}$$

such that P_{CMM} is the vector of X and Y locations for each hole in the grid plate in millimeters, and $P_{OrthoImage}$ is the vector of X and Y locations for each hole in the transformed orthogonal image of the grid plate in pixels. Therefore, Eq 4 implies that any image taken by the calibrated system can be transformed via Eq 1 & 2 and scaled by $\boldsymbol{S}$ to arrive at pixelated metered units in the image.

Permanent reference fiducials directly outside the build area are captured during the creation of both the transformation matrix and the scaling map (system calibration). These same fiducials are likewise captured in all subsequent measurements, and are used to orient all images in a consistent stationary global coordinate frame. Once calibrated, any image taken by the measurement system can then be transformed, scaled, and rotated into this coordinate frame. In this fashion, the entire build area in each layer can be turned into pixelated data points in metered space.

2.2 Digital Fringe Projection System

The measurement of the area height profile is carried out via the projection of light with sinusoidally varying spatial intensity and a traditional phase shifting algorithm. The intensity distributions generated by the DLP projector on the power bed can be expressed as

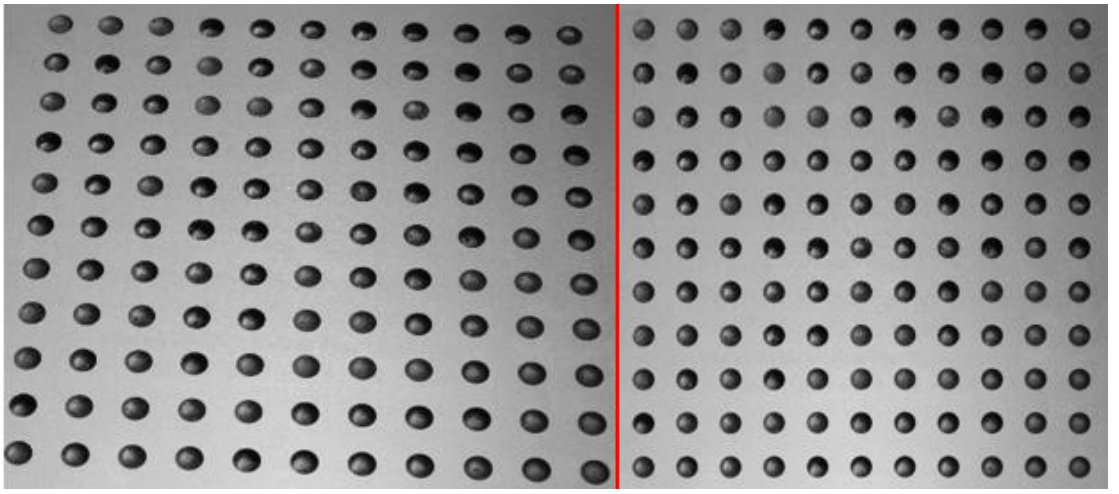

Figure 2: Left is the unaltered image of the calibration grid artifact taken by the imaging system during lateral calibration. The right is the same image in orthogonal space after perspective warping has been removed via planar projection transformation (1).

$$I_1(x,y) = I_0(x,y) + I_m(x,y) \cdot \cos\big(\phi(x,y)\big) \tag{5}$$

$$I_2(x,y) = I_0(x,y) + I_m(x,y) \cdot \cos\left(\phi(x,y) + \frac{\pi}{2}\right) \tag{6}$$

$$I_3(x,y) = I_0(x,y) + I_m(x,y) \cdot \cos(\phi(x,y) + \pi) \tag{7}$$

$$I_4(x,y) = I_0(x,y) + I_m(x,y) \cdot \cos\left(\phi(x,y) + \frac{3\pi}{2}\right) \tag{8}$$

where $I_i(x,y)$ is the intensity at each pixel in one of four pictures captured in the process, $I_0(x,y)$ is the offset intensity in the system, $I_m(x,y)$ is the modulation intensity, and $\phi(x,y)$ is the phase which is desired to be known at each pixel. Solving equations 5 through 8, we obtain the phase as defined by Eq 9, below.

$$\phi(x,y) = tan^{-1}\left(\frac{I_4(x,y) - I_2(x,y)}{I_1(x,y) - I_3(x,y)}\right) \tag{9}$$

Through a calibration process, this relative phase information can be turned into relative height information by,

$$h(x,y) = \lambda_{eff}(x,y) \cdot \phi(x,y) \tag{10}$$

where $\lambda_{eff}(x,y)$ is called the effective wavelength at each pixel. It is defined as height change per fringe cycle, and is the output of the calibration procedure [Zhang, 2006].

The height information produced must be of sufficient resolution to accurately and robustly resolve the anticipated height drop of nearly 40 micrometers used in determining the solid-powder boundary. The most important factors in determining the resolution of the height map is the spatial frequency of the projected fringes onto the build plane, and the geometric arrangement of the imaging hardware. The placement of hardware in this case is largely dictated by the chamber size and available space given the many integrated sensors and ancillary equipment. Likewise, the ability to increase the spatial frequency of projected fringes is limited by the pixel density of the projector in use. It is beneficial to have several pixels per span of greyscale intensity in the fringe pattern to minimize noise and aliasing within the output phase map [Yashuiko, 1999].

2.3 Combining Area Height Profiles with Lateral Measurements

Once both calibrations are complete, fringes can be projected, shifted and imaged for each build layer, and a height map of the fused and un-fused powder surface can be created. Using the machine vision procedure outlined in Section 2.1, each pixel within the build area can be assigned lateral (X, Y) position relative to the global coordinate frame established by the reference marks immediately outside the build area. Once the sintered region is determined through relative height change, a layer-wise point cloud of the part being produced is obtained. Using the global coordinate references and data from the vertical stages within the chamber, each layer of data points can then be stacked together in post-processing to produce a 3D point cloud that represents the part produced in its entirety, including all obscured features once it is in final form. This high density 3D point cloud is the major output of the measurement system, and can be imported into a variety of modeling and analytical software for analysis.

3 Preliminary Measurement Results

3.1 Lateral Calibration of the Metrology System

As noted, after the appropriate transformation matrix and map of linear scaling factors have been established, they can be applied to subsequent images from the same stationary system. Post calibration imaging, the grid plate is removed from the chamber, and powder is introduced. The linear stages within the chamber bring the powder bed level with the focal plane of the lasing system. This coincides with the plane of system calibration; and matching the planes of powder bed, laser focus, and calibration is necessary for both quality sintering and measurement. Once the layer of powder has been sintered, an image of the entire build area is captured, including the aforementioned reference fiducials immediately outside the build area used in global coordinate registration. The image is then transformed into orthogonal space, and the entire image is passed through the linear mapping from pixels to metered units.

Since the map only has scaling factors at the locations and pitch of the grid plate artifact, each pixel undergoes a bi-linear interpolation within the map to determine the approximate scaling at every pixel location. The mapping of pixel coordinates to metered space is carried out independently for the X and Y directions respectively, each having their own scaling maps. Below, in Figure 3, is a visualization of the lateral errors seen in the uncalibrated image space as compared to the calibration grid plate's measurement by tactile CMM. These special distortions are removed through the application of the X and Y scaling map.

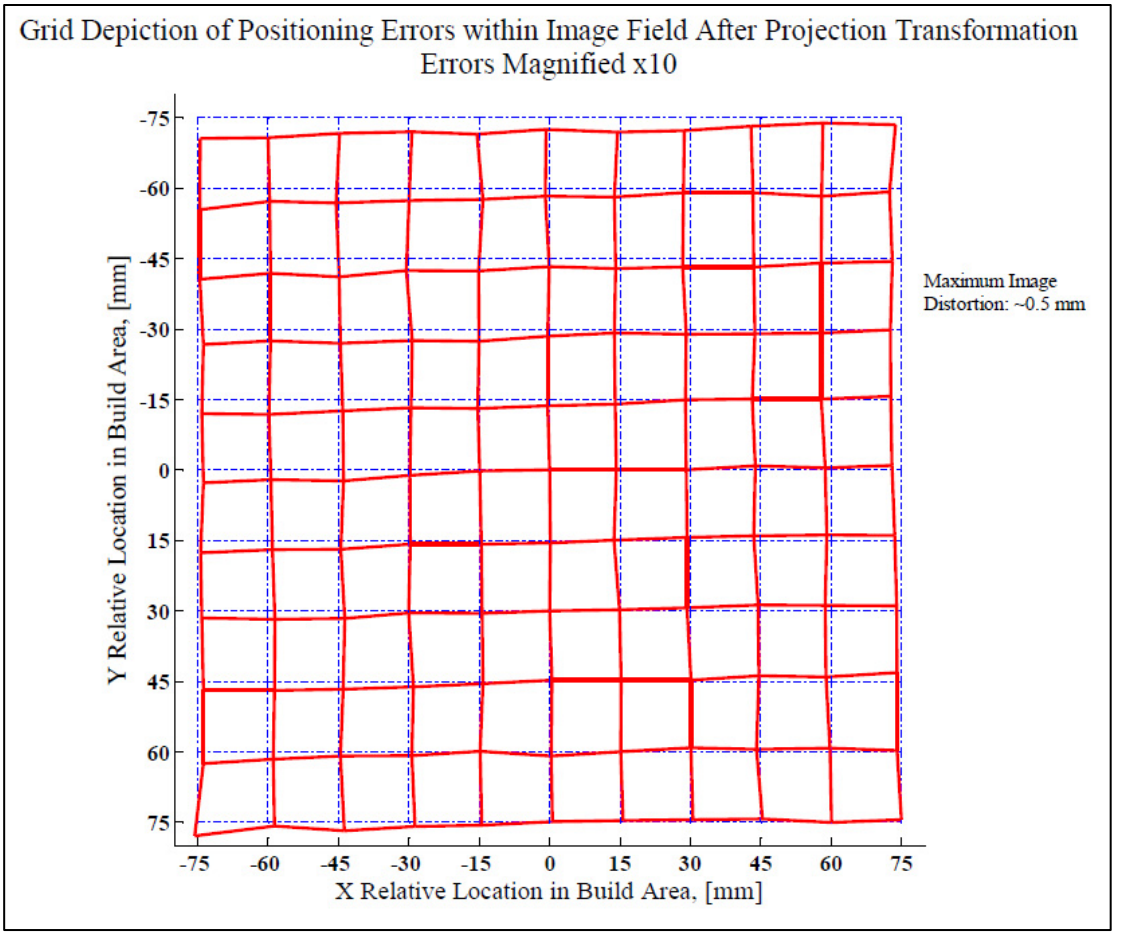

Figure 3: A visualization of the lateral spatial distortions seen in the uncalibrated image of the grid plate reference artifact. The intersections of the red lines depict the locations of each hole in the grid plate within the camera image as compared to the blue lines which are their locations as measured by a CMM. Note, the difference in hole position is magnified tenfold for graphical purposes.

3.2 Vertical Calibration of Metrology System

As described in Section 2.2, the conversion of relative phase to a relative height measurement requires the calculation of an effective wavelength. This procedure is called effective wavelength calibration and requires a diffuse flat plate as a reference artifact and a vertical motion translation stage. [Hoang, 2010] By counting the number of fringe shifts at the center of the flat plate while recording the corresponding height change, the effective wavelength is a simple ratio of the two. However, this approach is only capable of roughly estimating the effective wavelength of the system. A more accurate calibration involves capturing phase at each step height and mapping the effective wavelength at each pixel over the whole field of view [Purcell, 2006].

During the calibration, the plate is translated vertically above and below the build plane in equal increments by the translation stage. Calibration within the fusion chamber consisted of a 1 mm height

range centered around the build plane where incremental steps of 0.1 mm were used to generate the effective wavelength calibration. At each height location, phase shifting and phase unwrapping techniques are applied to obtain the initial phase within the build area. Then the slope of height per initial phase is derived by a least squares fitting of a line at each pixel as shown in Figure 4. In addition, all images used in the calibration process capture the permanent reference marks immediately outside the build area to allow registration to the global coordinate system, which allows for future association to the lateral measurement.

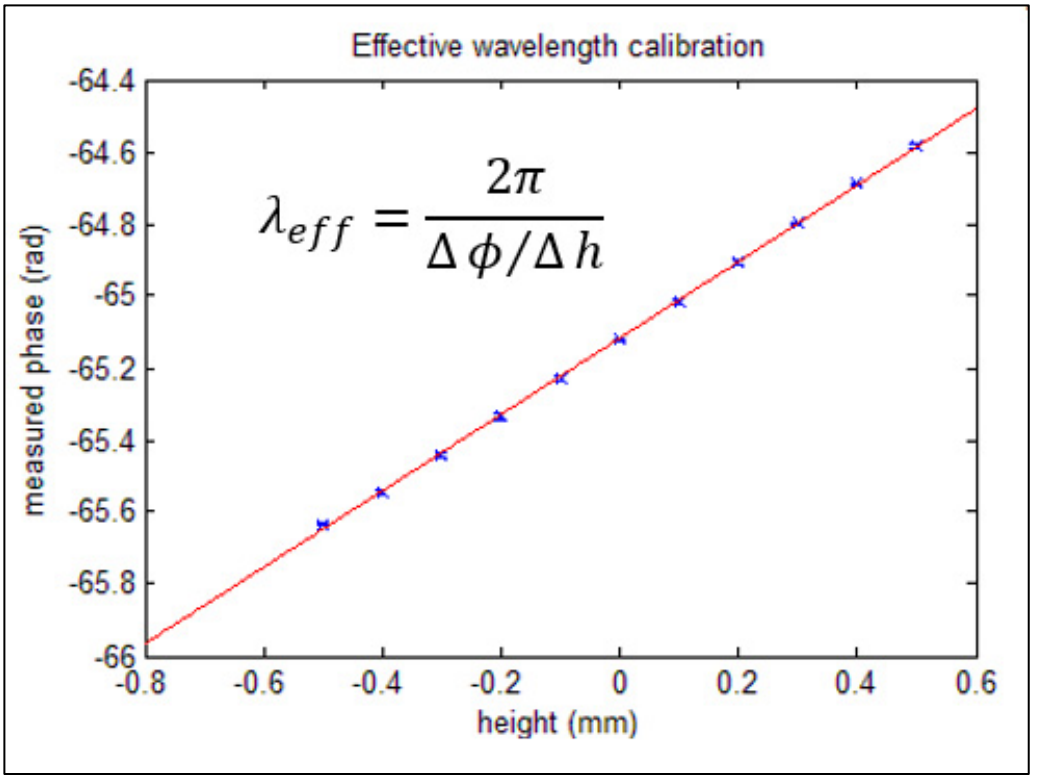

Figure 4: An example of the calculation of the effective wavelength for one pixel within the measurement image space. The figure shows the change in phase on the vertical scale of a single pixel as the vertical translation stage moves the calibration flat through a height range on the horizontal scale. The effective wavelength is shown as two pi divided by the slope of a least squares line fit to the tracked phase change.

3.3 In-Situ Height Measurements of Build Area

The first functionality tests of the metrology system within the laser fusion chamber were carried out on a simplistic build of two square prisms with a side length of one centimeter, offset from each other by two centimeters. An example image of a build layer from the metrology system is shown below in Figure 5. Images of the build were captured at various instances within the build cycle, allowing the powder bed surface to be characterized after a new layer of powder was laid, and after a round of laser fusion was completed. Due to software integration problems and general complications

in what was the first integrated testing of the metrology system, not all layers in the build were imaged nor were all steps in the build process captured as desired.

Height maps of over 15 build layers were generated and analyzed. Examples of several are shown in Figures 6 & 7. A noise floor of approximately 18 μm was achieved in the vertical measurement, which allows for reasonable recognition of sintered area depths and surface features. It should be noted that the below height maps have not been passed through the localized lateral scaling maps described above, and therefore exhibit some lateral distortion errors in their representation of XY space.

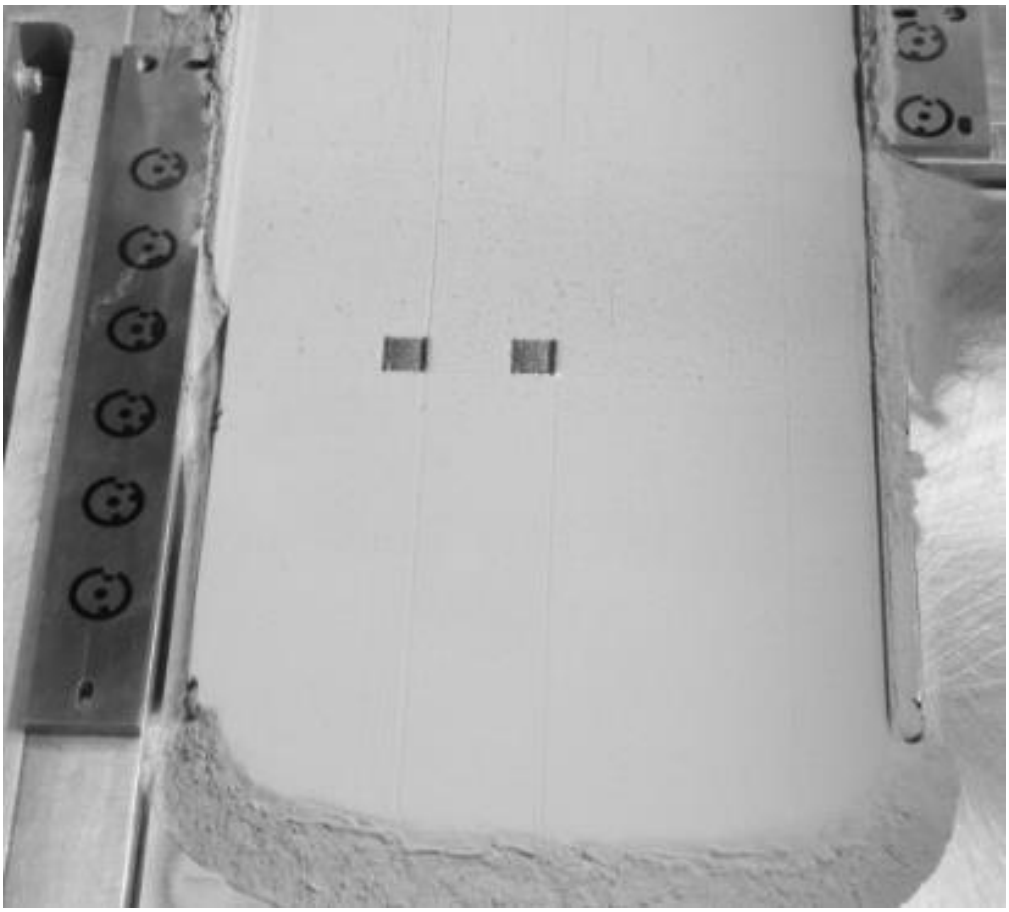

Figure 5: An example of the calculation of the effective wavelength for one pixel within the measurement image space. The figure shows the change in phase on the vertical scale of a single pixel as the vertical translation stage moves the calibration flat through a height range on the horizontal scale. The effective wavelength is shown as two pi divided by the slope of a least squares line fit to the tracked phase change.

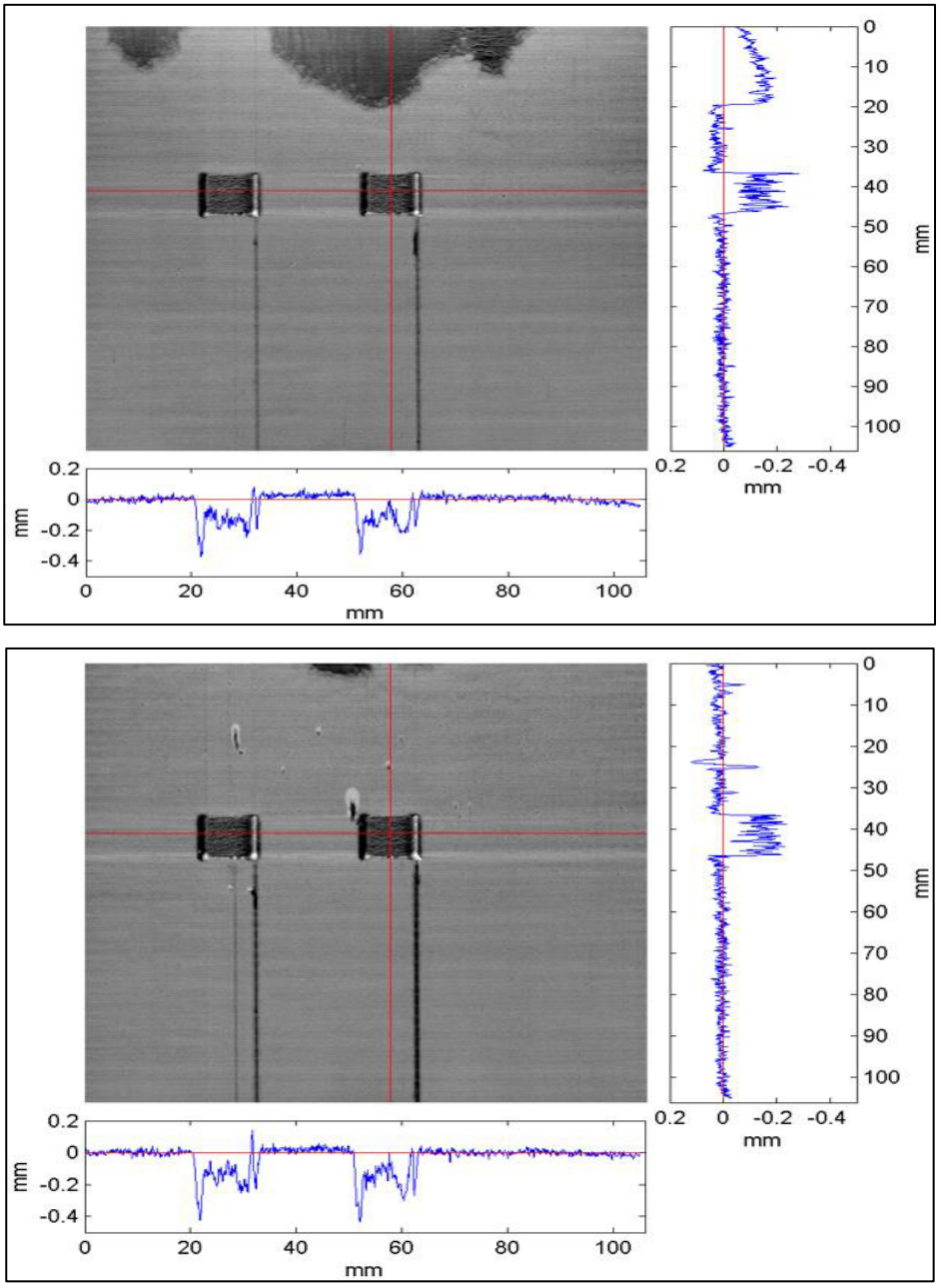

Figures 6 & 7: Height maps of build layers 8 and 10 are shown as examples of metrology system data output. A portion of the imaged build area is shown as a height map in grey scale with vertical and horizontal line profiles shown at right and bottom.

5 Future Work

Analysis of the data collected from the preliminary metrology system testing within the build chamber is ongoing. A second measurement trip to the EWI facility is in the planning phases where more data of various build types will be collected. Additionally, improvements are being made to the measurement procedure to produce a more accurate and robust measurement of the powder surface. A full uncertainty analysis on the measurement system is underway, with the aim of identifying major contributors and improving measurement fidelity. Long term goals include optimization of equipment and process parameters to produce quality measurements at levels of uncertainty far below the state-of-the-art capabilities of commercially available laser fusion systems. Also, the measurement of each layer is desired to be included in closed-loop control of the sintering process in real-time. Therefore, improving the speed of the process and compressing the amounts of data into actionable signals are goals for the second year of the project, along with the associated software development. Finally, the information collected from the metrology system described herein is aimed to be combined with data from an array of sensor systems developed by other collaborators to better understand the laser fusion process and how it might be improved.

6 Acknowledgements

This work is supported by funding from the National Institute of Standards and Technology, America Makes, and the Edison Welding Institute.

References

Arai, Y., Yokozeki, S. (1999). Improvement of measurement accuracy in shadow moiré by considering the influence of harmonics in the moiré profile. *Applied Optics*. 38(16). 3053-3057.

Hoang, T., Pan, B., Nguyen, D., Wang, Z. (2010). Generic gamma correction for accuracy enhancement in fringe-projection profilometry. *Optics Letters*. 35(12). 1992-1994.

Purcell, D. et al. (2006). Effective wavelength calibration for moire fringe projection, *Applied Optics*. 45(34). 8629-8635.

Wolberg, G. (1994). Digital Image Warping. *IEEE Computer Society Press*, Los Alamitos, CA, USA, p. 41-56

Zhang, S., Huang, P, (2006). Novel method for structured light system calibration. *Optical Engineering*. 45(8).